Full Paper

The Influence of Doping Levels and Surface Termination on the Electrochemistry of Polycrystalline Diamond

*Matthew N. Latto, Gustavo Pastor-Moreno, D. Jason Riley**

School of Chemistry, University of Bristol, Cantock's Close, Bristol BS8 1TH, UK
*e-mail: Jason.Riley@bristol.ac.uk

Received: April 15, 2003
Final version: April 29, 2003

Abstract
The influence of surface chemistry and boron doping density on the redox chemistry of $Fe(CN)_6^{3-/4-}$ at CVD polycrystalline diamond electrodes is considered. It is demonstrated that for this couple both the doping density and the surface chemistry are important in determining the rate of charge transfer at the electrode/electrolyte interface. For hydrogen terminated CVD diamond metallic electrochemical behavior is always observed, even at boron doping densities as low as 7×10^{18} cm^{-3}. In contrast, the electrochemical behavior of oxygen terminated CVD diamond varies with doping density, a metallic response being observed at high doping density and semiconductor behavior at low doping density. It is shown that the results attained may be explained by a surface state mediated charge transfer mechanism, thus demonstrating the importance of controlling surface chemistry in electroanalytical applications of diamond.

Keywords: Diamond, Electrochemistry, Surface states, Cyclic voltammetry

1. Introduction

Microcrystalline diamond coatings produced via chemical vapor deposition represent an exciting new electrode material. The electrochemistry of diamond has been extensively studied [1 – 10]. In addition to the obvious advantages of mechanical strength and chemical stability [11], electrodes formed from diamond also display a large potential window [12]. These factors have led to diamond being a material of choice in a number of electroanalytical applications [13 – 17]. Despite this high-level of interest the mechanism of charge transfer at the diamond electrode/electrolyte interface remains poorly understood.

Diamond is a semiconductor with a bandgap of 5.47 eV [11]. In most electrochemical studies the diamond employed is p-doped using boron. Boron doping is generally achieved either by the introduction of molecules containing boron [18], for example B_2H_6, to the CVD chamber during growth or by post-growth ion implantation [19]. It has been demonstrated that when boron is introduced during the growth process the doping density of CVD diamond films is directly proportional to the ratio of born to carbon in the feed gas [18]. The majority of electrochemical studies of boron doped CVD diamond (BDCD) have been concerned with samples prepared in which the boron to carbon ratio in the feed gas is greater than 100 ppm, which corresponds to a doping density greater than 10^{19} cm^{-3}. Fundamental electrochemical studies of such electrodes fall in to two categories; impedance investigations in indifferent electrolyte and cyclic voltammetric characterization using standard redox couples.

Several groups have reported capacitance studies of BDCD electrodes in indifferent electrolyte [2, 4, 20, 21]. The data obtained indicate that the applied potential is dropped across the space charge region, with plots of $1/C_{SC}^2$ against applied potential that are linear. This Mott-Schottky behavior suggests that even at the high boron levels employed in the literature the BDCD electrodes are not degenerately doped. In addition, the studies indicate that the flatband potential of BDCD electrodes is dependent upon surface termination. For hydrogen terminated BDCD surfaces the flatband potentials are reported to be independent of pH and lie in the range 0.5 to 0.75 V [2,4,21] versus a saturated calomel electrode (SCE). While in studies of oxygen terminated BDCD electrodes flatband potentials in the range 1.0 V to 4.0 V [20, 21] versus SCE have been reported. Some groups have stated that the flatband potential of oxygen terminated diamond is pH dependent while others claim that pH does not influence measurements. Further, there is evidence that the flatband potential of oxygen terminated samples is dependent upon the method employed to achieve the oxidation. The large difference in flatband potential between oxygen and hydrogen terminated BDCD electrodes, which has been explained in terms of the surface bond polarization, indicates that it is important to consider the surface termination when discussing BDCD electrochemistry.

Electrochemical studies of hydrogen terminated high doped BDCD using redox species that undergo outer sphere electron transfer reactions have been reported [1, 2, 20]. Cyclic voltammetric investigations at as-prepared electrodes report *j-V* curves that display both anodic and cathodic

  DOI: 10.1002/elan.200302857

peaks. Semimetallic behavior is also observed even for those redox couples that are electrochemically active in the depletion regime, i.e., those couples that possess a formal redox potential in the diamond bandgap. For high doped oxygen terminated samples semimetalic behavior is again reported. Studies of electron transfer kinetics at as-prepared and oxygenated electrode surfaces suggest that the electron transfer rates are faster at the former [22].

A mechanism of charge transfer at the BDCD electrode/electrolyte interface must account for the fact that both semiconductor, Mott-Schottky plots, and semimetal, anodic and cathodic peaks, behavior is observed. Below possible mechanisms of charge transfer at the BDCD electrode/electrolyte interface are discussed. In particular equations are developed that describe charge transfer via surface states at a BDCD/electrolyte interface. Results of experiments on charge transfer to the $Fe(CN)_6^{3-/4-}$ redox at low-doped BDCD electrodes are then detailed. The data obtained is discussed with reference to the different models presented for charge transfer at the BDCD electrode/electrolyte interface. It is shown that the surface state mediated charge transfer mechanism is able to account for all the results obtained.

2. Theory

Electrochemistry at semiconductor electrodes is usually discussed in terms of the Marcus-Gerischer model [23–26], this assumes iso-energetic electron transfer across the electrode/electrolyte interface. The theory as applied to charge transfer between a non-degenerately doped p-type semiconductor and a redox couple possessing a formal cell potential in the bandgap is outlined in brief below; more detailed discussion can be found in [23–26]. In the Marcus-Gerischer model for the as defined system the current depends on the overlap integral between the occupied/unoccupied states at the valence and conduction band edges and the unoccupied/occupied states of the redox system. In the case of diamond the conduction band edge is at such high energy, hydrogen terminated diamond has a negative electron affinity, that for redox couples in aqueous solution there is insignificant overlap between it and the energy levels of the electrolyte. Hence, here we focus on the overlap integrals between the valence band levels of the semiconductor and the redox states. Figure 1a is a schematic of the position of the relevant energy levels. For a non-degenerately doped semiconductor under depletion conditions a change in applied potential is manifested by a change in the potential drop across the space charge region. Figure 1b displays the semiconductor/electrolyte interface when a positive overpotential is applied. It is apparent that a positive overpotential leads to a reduction in band bending at the electrode surface and an increase in the surface density of holes. The surface density of holes varies exponentially with the applied potential, hence at the p-type semiconductor/electrolyte interface the anodic current increases exponentially with positive overpotential. In contrast the cathodic current, hole injection from the redox couple into the valence band, is essentially independent of the applied potential, the overlap integrals being invariant with potential. The interface between a non-degenerate semiconductor and a solution containing a redox couple with a formal cell potential in the bandgap has been

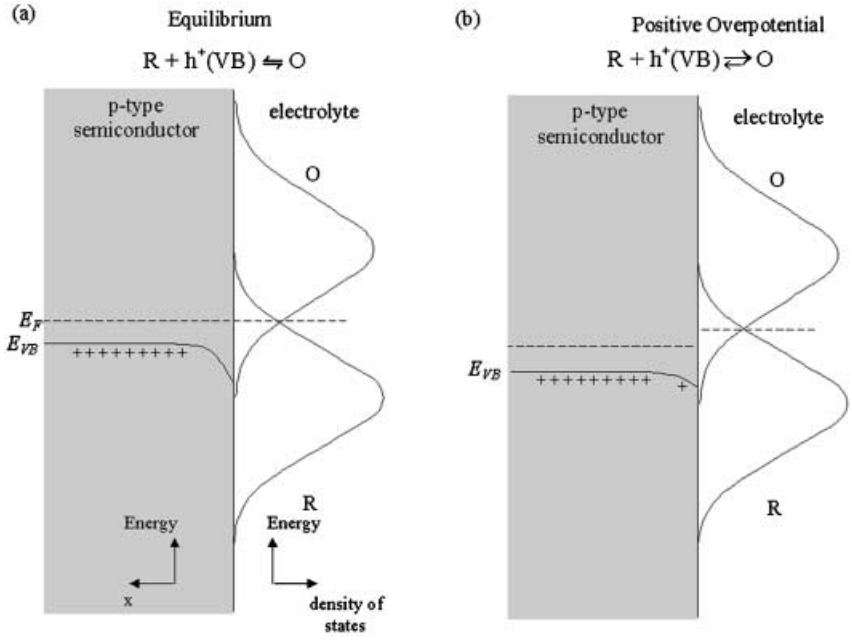

Fig. 1. A schematic representation of the electronic levels of an ideal p-type semiconductor and a simple redox system; a) under equilibrium conditions when the Fermi level, E_F, of the redox system is equal to that of the semiconductor, b) under forward bias.

compared to a Schottky diode, with low constant current at reverse bias and current that increases exponentially under forward bias.

Deviations from the semiconductor electrode behavior detailed above, which is often termed ideal, may stem from either degenerate doping of the semiconductor or the presence of surface states. For a highly doped p-type semiconductor the Fermi level may lay within the valence band, such a semiconductor is referred to as being degenerately doped. As there is a density of states about the Fermi level such electrodes behave in a similar manner to metal electrodes; dropping most of the applied potential across the Helmholtz layer and yielding cyclic voltammograms that show anodic and cathodic peaks. Surface states may alter the electrochemical response of a semiconductor/electrolyte interface by mediating the charge transfer process. The surface states mediated charge transfer process involves consecutive tunnelling events, between the bulk semiconductor and the surface states and between the surface states and the electrolyte. Although charge transfer via surface states is often invoked to explain facile charge transfer at semiconductor electrodes, indeed it has been postulated for BDCD electrodes [2, 27], comprehensive descriptions of the mechanism are limited. In a detailed analysis Vanmaekelbergh [28, 29] discusses the potential dependence of all four steps in the surface mediated charge transfer process; forward and reverse electron transfer between the bulk semiconductor and the surface state and forward and reverse electron transfer between the surface state and the solution phase redox species. Vanmaekelbergh has employed the theory to explain the current versus potential curves obtained at a boron doped, single crystal diamond electrode [20]. Chazalviel [30] has developed a simplified model of an n-type semiconductor/electrolyte which assumes that current flowing across the Helmholtz layer can be derived from Marcus theory [23, 24] while the charge across the space charge region can be described using Schottky diode theory [31]. To facilitate the calculation of the current density as a function of potential his model only considers interfaces for which the Helmholtz layer capacitance, C_H, is orders of magnitude greater than the space charge layer capacitance, C_{SC}. Below we develop the latter approach for p-type BDCD electrodes, taking into account that a fraction of the applied potential may be dropped across the Helmholtz layer. The aim is to develop equations that qualitatively describe the influences of doping density and surface state density on the rate of electron transfer.

Figure 2a is a schematic of the semiconductor/surface states/redox couple at equilibrium. The Fermi level for the bulk semiconductor, the surface states and the solution phase redox couple lies at a common energy, $E_{e,0}$. The situation when a positive potential of magnitude δV is applied is shown in Figure 2b. The applied bias is dropped across the space charge layer, δV_{SC}, and the Helmholtz layer, δV_H. The applied bias results in a change in the energy distribution of electrons in the surface state. If it is assumed that, even under non-equilibrium conditions, the electrons in the surface states obey Fermi statistics, i.e., they are thermalized, then the change in the energy may be expressed as δE_0. Assuming i) that Marcus-Gerischer theory for electron transfer between the surface states and the redox couple is valid, ii) a transfer coefficient of 0.5 and iii) the absence of concentration polarization, the expression for the current density across the Helmholtz layer, j_H, is

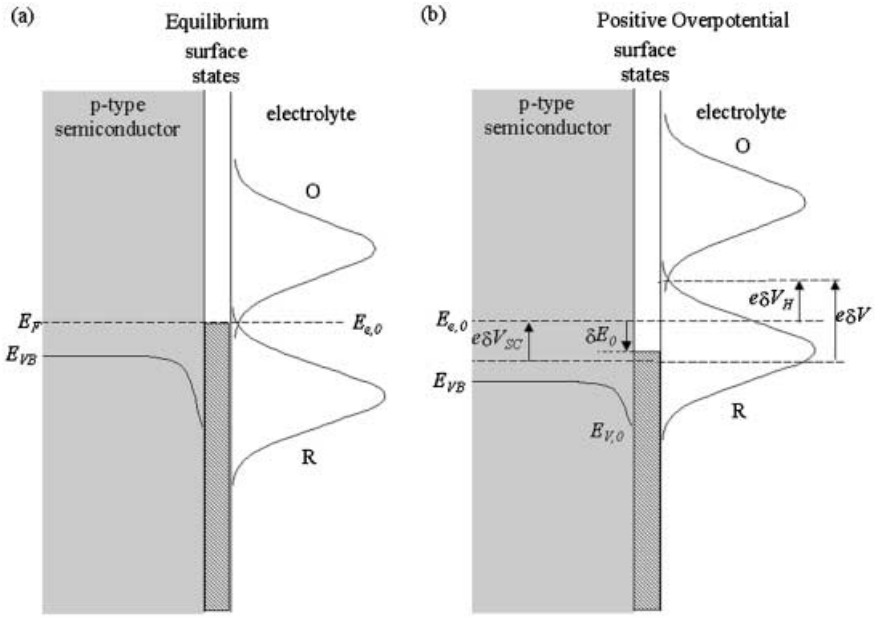

Fig. 2. A schematic representation of the electronic levels of a p-type semiconductor with a uniform density of surface states and a simple redox system; a) under equilibrium conditions when the Fermi level, E_F, of the redox system is equal to that of the semiconductor; b) under a forward bias, δV.

$$j_H = 2j_{H,0}\left(\sinh\left(\frac{e\delta V_H - \delta E_0}{2kT}\right)\right) \quad (1)$$

where e is the modulus of the charge on an electron, k is Boltzmann's constant, T is the temperature and $j_{H,0}$ is the exchange current density across the Helmholtz layer. Assuming that the boundary between the bulk semiconductor and the surface states can be modelled as a Schottky barrier the current across this junction, j_{SC}, is

$$j_{SC} = j_{SC,0}\exp\left(-\frac{\delta E_0}{kT}\right)\left(\exp\left(\frac{e\delta V_{SC} + \delta E_0}{kT}\right) - 1\right) \quad (2)$$

where $j_{SC,0}$ is given by the expression

$$j_{SC,0} = A * T^2 \exp\left(\frac{E_{V,0} - E_{e,0}}{kT}\right) \quad (3)$$

in which A^* is the Richardson constant for thermionic emission for hole capture from surface states and $E_{V,0}$ is the energy of the valence band edge. Applying Kirchoff's law to the electrode/electrolyte interface yields

$$j = j_{SC} + C_{SC}\frac{dV_{SC}}{dt} = j_H + C_H\frac{dV_H}{dt} \quad (4)$$

where j is the current, C_{SC} the capacitance across the space charge layer and C_H the Helmholtz capacitance. As the applied potential is the sum of the space charge and Helmholtz potentials Equation 4 can be written as:

$$\frac{dV_H}{dt} = (1-\gamma)\frac{dV}{dt} + \left(\frac{1}{C_H + C_{SC}}\right)\frac{dQ_{ss}}{dt} \quad (5)$$

where γ is $C_H(C_H + C_{SC})$ and Q_{ss} is the charge on the surface states. If the density of surface states per eV is $\rho(E_0)$ then $dQ_{ss} = -e\rho(E_0)dE_0$. Hence if C_H, C_{sc} and $\rho(E_0)$ are potential independent, i.e., the density of surface states is uniform, the expressions for δV_H and δV_{SC} are

$$\delta V_H = (1-\gamma)\delta V - \beta\delta E_0 \quad (6)$$

and

$$\delta V_{SC} = \gamma\delta V - \beta\delta E_0 \quad (7)$$

where $\beta = e\rho(E_0)/(C_H + C_{SC})$. Eliminating δE_0, δV_{SC} and δV_H from Equations 1 and 2 yields

$$j_{SC} = j_{SC,0} \times \exp\left(-\frac{e}{(\beta+1)kT}\left[(1-\gamma)\delta V - \frac{2kT}{e}\sinh^{-1}\left(\frac{j_H}{2j_{H,0}}\right)\right]\right) \times \left(\exp\left(\frac{e}{kT}\left[\delta V - \frac{2kT}{e}\sinh^{-1}\left(\frac{j_H}{2j_{H,0}}\right)\right]\right) - 1\right) \quad (8)$$

When for a particular potential a steady-state current is achieved $j_{SC} = j_H = j$ and Equation 8 may be written as

$$j = j_{SC,0} \times \exp\left(-\frac{e}{(\beta+1)kT}\left[(1-\gamma)\delta V - \frac{2kT}{e}\sinh^{-1}\left(\frac{j}{2j_{H,0}}\right)\right]\right) \times \left(\exp\left(\frac{e}{kT}\left[\delta V - \frac{2kT}{e}\sinh^{-1}\left(\frac{j}{2j_{H,0}}\right)\right]\right) - 1\right) \quad (9)$$

For a range of overpotentials the iterative Levenberg-Marquardt method [32] allows values of j to be found that satisfy the above equality. However, it is instructive to consider the limiting case that $C_H >> C_{SC}$, i.e., $\gamma = 1$, Equation 9 then reduces to

$$\delta V = \frac{2kT}{e}\sinh^{-1}\left(\frac{j}{2j_{H,0}}\right) + \frac{kT}{e} \times \ln\left[1 + \frac{j}{j_{SC,0}}\exp\left(-\frac{2}{e\beta+1}\sinh^{-1}\left(\frac{j}{j_{H,0}}\right)\right)\right] \quad (10)$$

This implies that for high β the total current density is the sum of currents across the space charge region and that across the Helmholtz layer. Under such conditions current-voltage behavior will be symmetric about $\delta V = 0$ for $j_{SC,0} >> j_{H,0}$, i.e., when charge transfer from the surface states to the redox species is the rate limiting step, and will show Schottky behavior for $j_{SC,0} << j_{H,0}$, i.e., when electron transfer across the space charge layer is rate limiting. The situation for lower values of β is more complex as the current across the space charge layer is dependent on both the number of surface states and the current across the Helmholtz layer. For diamond electrodes in depletion Mott-Schottky plots imply C_{SC} is of the order of 0.1 μF cm^{-2} and impedance analysis [4] yields values of C_H of approximately 1 μF cm^{-2} suggesting that $\gamma = 0.9$. Figure 3 shows solutions to Equation 9 for $\gamma = 0.9$ and $j_{H,0} = 1 \times 10^{-6}$ μA cm^{-2} [20]. For simplicity the influences of the parameters β and $j_{SC,0}$ are considered separately, it should be noted that $j_{SC,0}$ will be directly proportional to the density of surface states, the probability of hole injection increasing with increased surface state density. However, information that would permit an estimation of the constant of proportionality for diamond is not available. In Figure 3a Tafel plots are displayed for $j_{SC,0} = 5 \times 10^{-3}$ μA cm^{-2} and varying β, i.e., density of surface states. It is apparent that at high

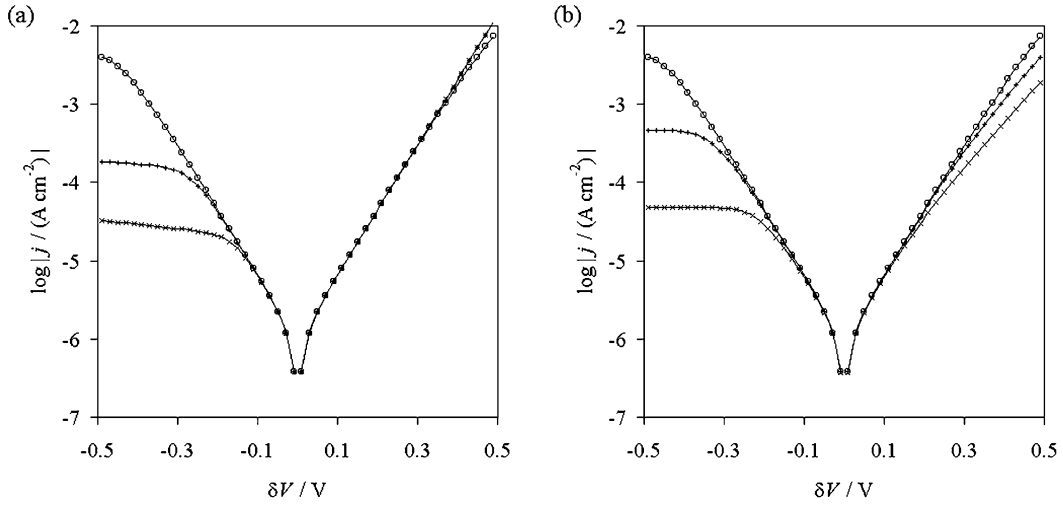

Fig. 3. Calculated current-potential characteristics for surface state mediated charge transfer from a p-type semiconductor to a simple redox couple. Both plots were calculated assuming $j_{H,0} = 1 \times 10^{-6}$ A cm^{-2} and $\gamma = 0.9$. For plot (a) $j_{SC,0} = 5 \times 10^{-3}$ A cm^{-2} and β is 10^{21} (○), 10^{19} (+) or 10^{17} (×). For plot (b) $\beta = 10^{21}$ and $j_{SC,0}$ is 5×10^{-3} A cm^{-2} (○), 5×10^{-4} A cm^{-2} (+) or 5×10^{-5} A cm^{-2} (×).

surface state density, assuming $C_H + C_{SC}$ is 1 μF cm^{-2} a β of 10^{21} corresponds to a density of surface states of 10^{15} cm^{-2} eV^{-1}, a symmetric current voltage plot is observed. However, as the density of surface states is reduced to 10^{13} cm^{-2} eV^{-1} and 10^{11} cm^{-2} eV^{-1} the cathodic current is limiting. Current-voltage curves for $\beta = 10^{21}$ and differing values of $j_{SC,0}$ are depicted in Figure 3b. It is apparent that the electrode/electrolyte junctions begins to act as a Schottky diode as the density of surface states and/or the magnitude of $j_{SC,0}$ decreases.

3. Experimental

Undoped silicon ⟨100⟩ wafers approximately 1 cm by 2 cm in dimensions were employed as substrates for diamond growth. The substrates were manually abraded with 1–3 μm diamond grit and BDCD deposited using a hot filament reactor. High doped BDCD films were grown at a pressure of 20 Torr and flow rates of 200 sccm (cm^3 as measured at standard temperature and pressure) of H_2, 1.4 sccm of CH_4 and 2×10^{-3} sccm of B_2H_6, yielding a boron to carbon ratio of approximately 3000 ppm in the gas phase. Assuming the B:C ratio in the as formed BDCD matches that in the gas phase this corresponds to a doping density of 10^{20} cm^{-3}. Low doped films were grown at a pressure of 20 Torr and typical flow rates were 200 sccm of H_2, 1.4 sccm of CH_4 and 4×10^{-5} sccm of B_2H_6. The low flow rate of the diborane was achieved by pre-dilution of the purchased diborane, a 4.75% premix of diborane in hydrogen from BOC, in more hydrogen. The flow rates employed indicate a boron to carbon ration of 50 ppm was present in the gas phase during growth, corresponding to a doping density of 10^{18} cm^{-3}. It should be noted that the CVD chamber was cleaned prior to preparation of low doped samples to minimize doping by the residual boron on the surfaces of the chamber. Deposition runs of 12 hours were employed to yield films of approximately 4 μm thickness. The film was allowed to cool in a hydrogen atmosphere before removal from the chamber. Prior to electrochemical studies the quality of the diamond was assessed using Raman spectroscopy and SEM, the results of such studies are published in reference [33].

Electrochemical experiments were performed on as-prepared boron doped CVD diamond samples, referred to as hydrogen terminated and on diamond electrodes that had been treated with boiling chromic acid, referred to as oxygen terminated [34, 35]. Three types of contact were employed in the studies. For high doped samples silver paint was used to adhere a copper wire directly to the diamond film. For the low doped samples Ohmic contacts were formed using metal carbides. On the oxygen terminated samples a three layer metal contact was deposited post oxidation [36]. Titanium was evaporated onto a corner of the electrode, this was then covered with sputtered platinum and evaporated gold before annealing in a vacuum at 500 °C. For the hydrogen terminated samples a titanium under-layer contact was employed, i.e., a thin strip of titanium evaporated on to the edge of the substrate prior to BDCD deposition. Full preparation and performance details of the latter type of contact are available in [37]. All contacts showed excellent linearity over the potential range of interest.

Electrochemical experiments were performed in a single compartment cell fabricated from PTFE. The BDCD working electrode was placed against a window at the base of the cell and the fluid contained using an O-ring. The geometric area of the working electrode exposed to electrolyte was 0.07 cm^2 and all currents are normalized against this value. A commercial Ag/AgCl/3 mol dm^{-3} Cl$^-$ electrode and a flame annealed platinum grid were employed as reference and counter electrode respectively. All potentials are quoted relative to the reference electrode. Cyclic

voltammograms were recorded using an Ecochemie μ-Autolab potentiostat and associated software.

All chemicals were reagent grade and used without further purification. The following solutions were prepared using 18 MΩ cm water (Millipore); 0.010 mol dm^{-3} $K_3Fe(CN)_6$ + 0.010 mol dm^{-3} $K_3Fe(CN)_6$ in 1.0 mol dm^{-3} KCl and 0.003 mol dm^{-3} $K_3Fe(CN)_6$ + 0.003 mol dm^{-3} $K_3Fe(CN)_6$ in 1.0 mol dm^{-3} KCl. The solutions were degassed for 20 minutes with nitrogen prior to electrochemical experiments.

4. Results and Discussion

The $Fe(CN)_6^{3-/4-}$ couple was studied as its redox potential lies within the bandgap of both oxygen and hydrogen terminated BDCD electrodes. Cyclic voltammograms, recorded at a scan rates of 25 mV s^{-1}, for the as-prepared BDCD electrodes in 0.010 mol dm^{-3} $K_3Fe(CN)_6$ + 0.010 mol dm^{-3} $K_3Fe(CN)_6$ in 1.0 mol dm^{-3} KCl. For the $Fe(CN)_6^{3-/4-}$ redox couple at the hydrogen terminated BDCD surface, Figure 4a, both anodic and cathodic peaks are observed. The peak separation is large, however, it must be noted that the low doping of the BDCD resulted in films of low conductivity and *iR* compensation was not used when recording the cyclic voltammograms. For the $Fe(CN)_6^{3-/4-}$ couple at the low doped oxygen-terminated BDCD surface, Figure 4b, a well defined anodic peak is observed but the cathodic peak is absent. This result is in contrast to the behavior of high-doped oxygen terminated BDCD, Figure 4c, where reversible behavior is observed using the same redox couple.

First we consider the response of the low doped oxygen terminated BDCD surface. At first sight the *j-V* curve obtained in Figure 4b suggests an ideal semiconducting electrode has been fabricated. However, Mott-Schottky analysis of the oxygen-terminated diamond immersed in 1 mol dm^{-3} KCl (not shown) yields a flat band potential of +1.7 V (vs. Ag/AgCl) while against the same reference the redox couple had an $E_{1/2}$ of 0.257 V. These values point to minimal overlap integrals between the energy levels of the $Fe(CN)_6^{3-/4-}$ in solution and the valence band edge of the BDCD and therefore negligible anodic current. Hence direct charge transfer from the valence band to the redox couple can be discounted. The low doping level employed and the fact that the *j-V* curve does not possess a well-defined cathodic peak indicate that the diamond is not degenerately doped. Hence, the only redox mechanism that is consistent with all the experimental data is surface state mediated charge transfer. The diode response in the *j-V* curve is indicative of a low density of surface states, i.e., low $j_{SC,0}$ and low β.

For the high doped oxygen terminated diamond, Figure 4c, the shape of the *j-V* curve indicates that direct charge transfer via the valence band can be discounted. The semimetallic redox signal is consistent with degenerate doping. However, given that the boron acceptor states have a high activation energy of 0.37 eV and only 0.01% of them

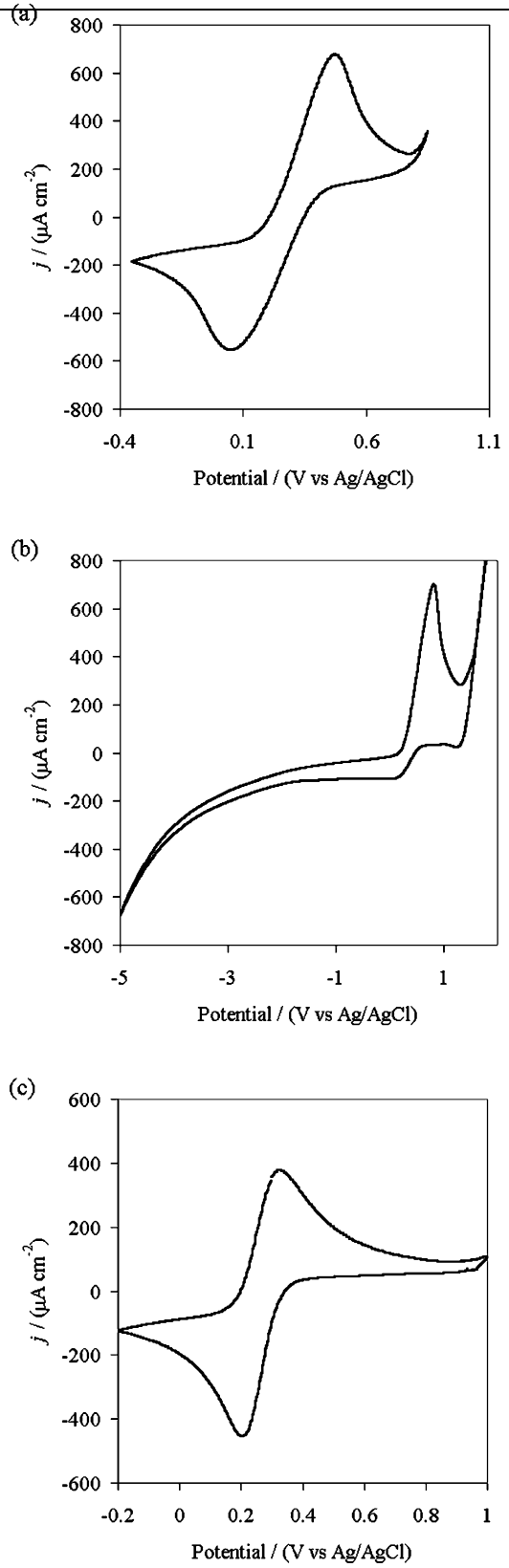

Fig. 4. Cyclic voltammetric *j-V* curves. a) Hydrogen terminated low doped BDCD in 0.010 mol dm^{-3} $Fe(CN)_6^{3-/4-}$ with 1.0 mol dm^{-3} KCl, scan rate = 25 mV s^{-1}. b) Oxygen terminated low doped BDCD in 0.010 mol dm^{-3} $Fe(CN)_6^{3-/4-}$ with 1.0 mol dm^{-3} KCl, scan rate = 25 mV s^{-1}. c) Oxygen terminated high doped BDCD in 0.003 mol dm^{-3} $Fe(CN)_6^{3-/4-}$ with 1.0 mol dm^{-3} KCl, scan rate = 20 mV s^{-1}.

are ionized [38] a doping level of $10^{20}\,cm^{-3}$ appears insufficient to produce a degenerately doped sample. The doping level is also below the limit, $10^{21}\,cm^{-3}$, at which overlap of impurity states leads to metallic conduction bands [39]. Further evidence for non-degenerate doping is supplied by Mott-Schottky analysis of the BDCD electrodes that indicate that the applied potential is dropped across the space charge region. Thus it appears the charge transfer process again must be mediated by surface states. In impedance studies [20, 40] of high doped oxygen terminated BDCD two time constants are observed, providing strong evidence for this mechanism. Comparison of the *j-V* curves for the redox chemistry at the oxygen terminated high doped and low doped BDCD indicates that the change in doping level leads to an increase in the density of surface states that participate in the charge transfer process. Hence, for oxygen terminated diamond it appears that it is the boron states that mediate the charge transfer between the bulk semiconductor and the redox couple.

The low doped hydrogen terminated BDCD, Figure 4a, shows markedly different electrochemical behavior to the oxygen terminated sample of the same doping density, Figure 4b. It has been established that hydrogen termination leads to increased free carrier density near the surface [41] and it has been postulated that the marked difference in electrochemical behavior between oxygenated and hydrogenated BDCD electrodes stems from a change from non-degenerate to degenerate doping [42]. However, this theory is not supported by the fact that impedance studies of hydrogen terminated BDCD diamond, even at high doping density, yield Mott-Schottky plots. For metal-BDCD Schottky junctions it has been shown that surface termination plays a vital role in determining the Schottky barrier performance [34, 38]. For oxygen terminated BDCD/metal interfaces it has been shown that the Schottky barrier can be described using a simple thermionic emission model. However, at junctions between hydrogen terminated BDCD and a metal the temperature dependence of the current indicates that tunneling across the barrier occurs and a thermionic-field emission model is required to model the characteristics of the junction. This implies that in the solid state case hydrogen acts as a low level acceptor state, increasing the number of free carriers and thinning the space charge barrier sufficiently for tunneling to occur between the bulk semiconductor and the metal. In the electrochemical model detailed above field emission across the barrier between bulk BDCD and surface states would lead to an increase in $j_{SC,0}$. It is apparent from Figure 3b that for the surface state mediated charge transfer mechanism a change in $j_{SC,0}$ is sufficient to alter the electrochemical behavior from semiconductor to semimetallic. This indicates that the results displayed in Figures 4a and 4b are consistent with the surface state mediated mechanism.

5. Conclusions

The experimental results indicate that both doping density and surface termination are important in determining the response of BDCD electrodes. The influences of these parameters on electrode behavior are consistent with a surface state mediated charge transfer mechanism. It appears that for oxygen terminated diamond a change in the doping density results in a change in the density of the boron surface states that mediate charge transfer. While a change in the surface chemistry, from oxygen to hydrogen terminated, leads to a change in free carrier concentration and in the mechanism of charge transfer, thermionic to field-thermionic, across the space-charge layer. In this paper the results are shown for extreme changes of doping density and surface chemistry. We note however that the model developed for surface state mediated charge transfer predicts slower electrode kinetics as the doping level decreases or the surface is oxidized, such behavior has been reported in the literature [22, 43].

6. Acknowledgements

The financial support of the EPSRC (GR/L84308) and the University of Bristol are gratefully acknowledged. We thank Dr. Paul W. May of the University of Bristol for help in fabricating the BDCD electrodes.

7. References

[1] J. W. Strojek, M. C. Granger, G. M. Swain, T. Dallas, M. W. Holtz, *Anal. Chem.* **1996**, *68*, 2031.
[2] S. Alehashem, F. Chambers, J. W. Strojek, G. M. Swain, R. Ramesham, *Anal. Chem.* **1995**, *67*, 2812.
[3] A. Y. Sakharova, Y. V. Pleskov, F. Diquarto, S. Piazza, C. Sunseri, I. G. Teremetskaya, V. P. Varnin, *J. Electrochem. Soc.* **1995**, *142*, 2704.
[4] Y. V. Pleskov, V. V. Elkin, M. A. Abaturov, M. D. Krotova, V. Y. Mishuk, V. P. Varnun, I. G. Teremetskaya, *J. Electroanal. Chem.* **1996**, *413*, 105.
[5] C. H. Goeting, J. S. Foord, F. Marken, R. G. Compton, *Diamond Relat. Mater.* **1999**, *8*, 824.
[6] C. H. Goeting, F. Jones, J. S. Foord, J. C. Eklund, F. Marken, R. G. Compton, P. R. Chalker, C. Johnston, *J. Electroanal. Chem.* **1998**, *442*, 207.
[7] C. Reuben, E. Galun, H. Cohen, R. Tenne, R. Kalish, Y. Muraki, K. Hashimoto, A. Fujishima, J. E. Butler, C. Levy-Clement, *J. Electroanl. Chem.* **1995**, *396*, 233.
[8] S. Nakabayashi, N. Ohta, A. Fujishima, *PCCP* **1999**, *1*, 3993.
[9] F. Bouamrane, A. Tadjeddine, R. Tenne, J. E. Butler, R. Kalish, C. Levy-Clement, *J. Phys. Chem. B* **1998**, *102*, 134.
[10] F. Bouamrane, A. Tadjeddine, R. Tenne, J. E. Butler, C. Levy-Clement, *J. Electroanal. Chem.* **1996**, *405*, 95.
[11] P. W. May, *Phil. Trans. R. Soc. Lond. A* **2000**, *358*, 473.
[12] H. B. Martin, A. Argoitia, U. Landau, A. B. Anderson, J. C. Angus, *J. Electrochem. Soc.* **1996**, *143*, L133.
[13] A. J. Saterlay, F. Marken, J. S. Foord, R. G. Compton, *Talanta* **2000**, *53*, 403.
[14] R. Uchikado, T. N. Rao, D. A. Tryk, A. Fujishima, *Chem. Lett.* **2001**, 144.

[15] M. C. Koppang, M. Witek, J. Blau, G. M. Swain, *Anal. Chem.* **1999**, *71*, 1188.
[16] B. V. Sarada, T. N. Rao, D. A. Tryk, A. Fujishima, *Anal. Chem.* **2000**, *72*, 1632.
[17] S. Jolley, M. Koppang, T. Jackson, G. M. Swain, *Anal. Chem.* **1997**, *69*, 4099.
[18] M. Werner, R. Job, A. Zaitzev, W. R. Fahrner, W. Seifert, C. Johnston, P. R. Chalker, *Phys. Stat. Sol. A* **1996**, *154*, 385.
[19] G. R. Brandes, C. P. Beetz, C. F. Feger, R. W. Wright, J. L. Davidson, *Diamond Relat. Mater.* **1999**, *8*, 1936.
[20] J. van de Lagemaat, D. Vanmaekelbergh, J. J. Kelly, *J. Electroanal. Chem.* **1999**, *475*, 139.
[21] T. N. Rao, D. A. Tryk, K. Hashimoto, A. Fujishima, *J. Electrochem. Soc.* **1999**, *146*, 680.
[22] M. C. Granger, G. M. Swain, *J. Electrochem. Soc.* **1999**, *146*, 4551.
[23] Y. Q. Gao, Y. Georgievskii, R. A. Marcus, *J. Chem. Phys.* **2000**, *112*, 3358.
[24] R. A. Marcus, *J. Chem. Phys.* **1956**, *24*, 966.
[25] H. Gerischer, *Z. Phys. Chem. N. F.*, **1961**, *27*, 48.
[26] H. Gerischer, *J. Phys. Chem.* **1991**, *95*, 1356.
[27] M. C. Granger, M. Witek, J. S. Xu, J. Wang, M. Hupert, A. Hanks, M. D. Koppang, J. E. Butler, G. Lucazeau, M. Mermoux, J. W. Strojek, G. M. Swain, *Anal. Chem.* **2000**, *72*, 3793.
[28] D. Vanmaekelbergh, *Electrochim. Acta* **1997**, *42*, 1121.
[29] D. Vanmaekelbergh, *Electrochim. Acta* **1997**, *42*, 1135.
[30] J. N. Chazalviel, *J. Electrochem. Soc.* **1982**, 129, 963.
[31] S. M. Sze, *Physics of Semiconductor Devices*, 2nd ed., Wiley Interscience, New York **1981.**
[32] J. J. More, B. S. Garbow, K. E. Hillstrom, *User's Guide to Minpack I*, Argonne National Laboratory publication ANL-80-*74*, **1980.**
[33] G. Pastor-Moreno, D. J. Riley, *Electrochim. Acta* **2002**, *47*, 2589.
[34] H. Kawarada, *Surf. Sci. Rep.* **1996**, *26*, 205.
[35] Y. Mori, H. Kawarada, A. Hiraki, *Appl. Phys. Lett.* **1991**, *58*, 940.
[36] C. Jany, F. Foulon, P. Bergonzo, R. D. Marshall, *Diamond Relat. Mater.* **1998**, *7*, 951.
[37] M. S. Alexander, M. N. Latto, P. W. May, D. J. Riley, G. Pastor-Moreno,, *Diamond Relat. Mater.* **2003**, *12*, 1460.
[38] K. Hayashi, S. Yamanaka, H. Watanabe, T. Sekiguchi, H. Okushi, K. Kajimura, *J. Appl. Phys.* **1997**, *81*, 744.
[39] K. Nishimura, K. Das, J. T. Glass, *J. Appl. Phys.* **1991**, *69*, 3142.
[40] M. N. Latto, D. J. Riley, P. W. May, *Diamond Relat. Mater.* **2000**, *9*, 1181.
[41] K. Hayashi, S. Yamanaka, H. Okushi, K. Kajimura, *Appl. Phys. Lett.* **1996**, *68*, 376.
[42] D. A. Tryk, K. Tsunozaki, T. N. Rao, A. Fujishima, *Diamond Relat. Mater.* **2001**, *10*, 1804.
[43] N. Vinokur, B. Miller, Y. Avyigal, R. Kalish, *J. Electrochem. Soc.* **1996**, *143*, L238.

